Machine Learning in FET-based Chemical and Biological Sensors: A Mini Review

Jae-Hyuk Ahn[+]

Abstract

This mini review summarizes some of the recent advances in machine-learning (ML)-driven chemical and biological sensors. Specific focus is on field-effect-transistor (FET)-based sensors with a description of their structures and detection mechanisms. Key ML techniques are briefly reviewed for an audience not familiar with the basic principles. We mainly discuss two aspects: (1) data analysis based on ML and (2) ML applied to sensor design. In conclusion, the challenges and opportunities for the advancement of ML-based sensors are briefly considered.

1. INTRODUCTION

Chemical and biological sensors have been used in a variety of fields, including basic research, medicine, medical diagnosis, and health monitoring. Label-free electrical detection based on field-effect transistors (FETs) have many advantages, such as high sensitivity, small size, and easy integration with electronic circuits [1]. Researchers work to improve the sensitivity and ensure ease of use of the FET-based sensors to extend their use in practical applications. One of the strategies to increase detection sensitivity is to incorporate nanomaterials such as nanoparticles, nanowires, and two-dimensional (2D) materials, which increase the surface-to-volume ratio of the FET channel or strengthen the catalytic effects to sense target molecules [2,3]. The FET-based sensors can be fabricated on a flexible substrate, enabling wearable applications to monitor the health status of humans [4].

Machine learning (ML) is a branch of artificial intelligence that provides computers with the ability to automatically learn from data, identify patterns, and make decisions without being explicitly programmed [5]. Recently, the advances in ML have been driven by three factors: improved computing power, data availability and appropriate algorithms [6]. These advances enable ML techniques to make accurate predictions based on large sets of
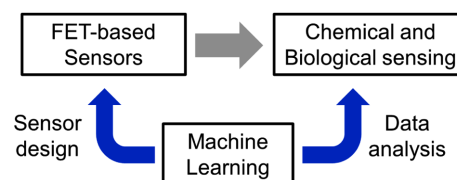
[1] Department of Electronics Engineering, Chungnam National Unversity, 99 Daehak-ro, Yuseong-gu, Daejeon 34134, Korea
[+] Corresponding author: jaehyuk@cnu.ac.kr

Fig 1. Scheme explaining how ML interacts with FET-based chemical and biological sensors in terms of sensor design and data analysis.

data [7].

ML enables researchers to analyze massive sensor data, assisting in designing experiments and new type of sensors [8]. Multidimensional data collected from an array of sensors are sometimes so complicated that humans have difficulty in analyzing them. However, ML algorithms are used to learn from data, recognize patterns, and classify the data. The ability to predict the result of new experiments can be utilized to design new high-performance sensors.

In this mini review, we discuss the effectiveness of ML to advance the technology associated with FET-based sensors (Fig. 1).

2. FET-BASED CHEMICAL AND BIOLOGICAL SENSORS

2.1 Structures

As shown in Fig. 2, a typical FET-based chemical and biological sensor is composed of a semiconducting material, two electrodes (source and drain) connected to the two ends, and a gate electrode that modulates the mobile charge carrier concentration within the
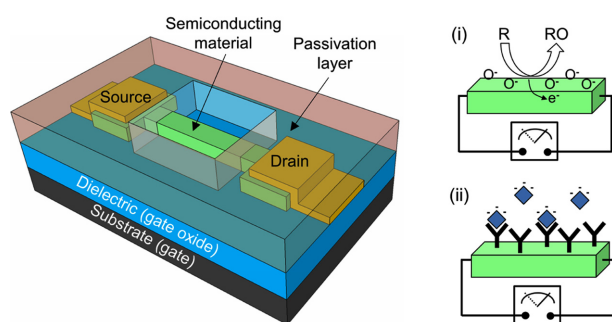
Fig 2. Schematic of an FET-based chemical and biological sensor. A semiconducting material is connected to source/drain electrodes and the current is controlled by the gate electrode. A passivation layer covers the sensor except the sensing area. For a gas sensor, analytes such as reducing gas molecules react with the oxygen absorbed on the semiconducting material and the electron transfer to the device occurs (i). For a biosensor, the surface is functionalized with receptors to capture analytes. The electrical current is affected by electrostatic interaction between analytes and semiconducting channel because of intrinsic charges of analytes bound on nanowire surface (ii).

semiconducting material by an electrical field effect through a gate dielectric, resulting in the electrical current. The semiconducting materials can be categorized into group IV semiconductors (i.e., Si and Ge) [9,10], III-V semiconductors (i.e., GaN and InP) [11], metal oxides (i.e., ZnO, In_2O_3, and SnO_2) [12], and conducting polymers (i.e., polyaniline and polypyrrole) [13]. The sensitivities of FET-based sensors can be increased by replacing channel materials with nanomaterials with high surface-to-volume ratios for the channel, such as nanowires, nanotubes, and 2D materials [14].

FET-based sensors typically have a bottom-gate structure where a handling substrate of silicon-on-insulator wafer (or a highly doped silicon substrate) is used as a gate. In this case, although the substrate for the sensor fabrication functions as a gate, and thus the fabrication of a gate electrode is simple, the individual addressing of multiple sensor devices becomes difficult due to a common gate structure. To overcome this problem, side gate configuration where gate electrodes are positioned beside the semiconductor materials is applied [15].

If semiconductor materials directly react with specific analytes, they can be utilized as sensors without additional surface functionalization. Otherwise, the surfaces of semiconductor materials are functionalized with receptors that selectively capture or react with target molecules. Receptors and catalytic nanomaterials decorated on the surface improve the specificity and sensitivity of the sensor by specific binding and catalytic interaction.

Biomolecular receptors including deoxyribonucleic acid (DNA), antibody, antigen, protein, and enzyme are used for the analyte detection based on specific binding and reaction. For antigen detection, nucleic acid aptamer as a receptor shows higher chemical stability than antibody. In gas sensors, catalytic nanoparticles (Pd, Pt, and Au) decorated on the FET surface accelerate the decomposition of gas molecules and react with the semiconductor channel, leading to higher sensitivity and selectivity.

The passivation layer surrounding the sensing area prevents unwanted chemical reactions. Particularly, in the case of biosensors operating in ionic solution, passivation layer should be covered on the metal electrodes or interconnection lines to prevent leakage current through the solution. Furthermore, materials used to prevent non-specific binding to the passivation layer enable biomolecules to focus on the sensing area and enhance sensitivity and detection limits.

2.2 Detection mechanisms

In FET-based sensors, the existence and concentration of target molecules can be recognized by monitoring the electrical characteristics such as conductance, resistance, and threshold voltage after the exposure to target species due to various mechanisms explained below.

2.2.1 Charge transfer

Primary mechanism of metal oxide nanowire-based gas sensors is the ionosorption of oxygen (Fig. 2). Oxygen absorbed on the surface of metal oxide nanowires (usually n-type nanowires) works as the surface state and receives electrons from the metal oxide nanowire to form O^- and O_2^- ions [16]. This charge transfer between oxygen and FET surface generates surface space charge (depletion region) in the semiconducting material, which increases the resistance. If reducing gas such as carbon monoxide (CO) removes the absorbed oxygen from the FET surface, electrons are released back to the semiconducting material and the resistance is decreased. The concentration of reducing gas is measured from the relationship between the resistance and partial pressure of the reducing gas.

Some gases react not only with absorbed oxygen ions but also with the atoms of the semiconducting material. The NH_3 or NO_2 molecules can penetrate the materials (especially conducting polymers) and function as electron acceptor and donor, respectively. As a result of charge transfer, the concentration of the electrical charge carrier is changed.

2.2.2 Electrostatic interaction

Electrical charge formed on the FET surface results in an electrostatic interaction, with electrical carriers flowing in the semiconducting channel, and affects the current or threshold voltage of the FET. For example, Pd nanoparticles decorated on the silicon nanowire decompose hydrogen molecules into hydrogen atoms, which then create a dipole layer on the surface, leading to the surface charge [15,17]. The dipole layer from hydrogen molecules is positively charged and thus attracts electrons in the n-type nanowire, resulting in an increase of the current, and decrease of the threshold voltage. The opposite effect occurs for the p-type nanowires.

In biosensors, target biomolecules are selectively bound to the nanowire surface through receptors, and the intrinsic charge of the biomolecules induces the surface charge (Fig. 2) [9,18]. For example, DNA molecules that are negatively charged due to the phosphate-deoxyribose backbone induce negative charge to the FET surface. Proteins express a certain net electrical charge depending on the combination of amino acids that are protonated or deprotonated at the given pH of the buffer solution. The pH value of the buffer solution at which the net charge of biomolecules becomes neutral is called the isoelectric point (pI). The biomolecules exhibit positive (negative) charge when surrounding pH is lower (higher) than pI. In other words, the polarity and amount of charge are determined by the pH of the buffer solution.

3. A BRIEF OVERVIEW OF ML

The two main types of ML are supervised learning and unsupervised learning [19]. In supervised learning, a set of labeled data is used for training. It means that the training dataset is tagged with the answer that should be the correct output. Supervised learning techniques are used for i) classification to group the output inside a class and ii) regression to predict a single output value using the training dataset. By contrast, unsupervised learning operates with unlabeled training dataset, which is a collection of examples without a correct answer. The most common unsupervised learning algorithm is clustering; it groups similar data points into clusters.

3.1 Principal component analysis

Principal component analysis (PCA) is one of the unsupervised ML techniques used for dimensionality reduction, feature
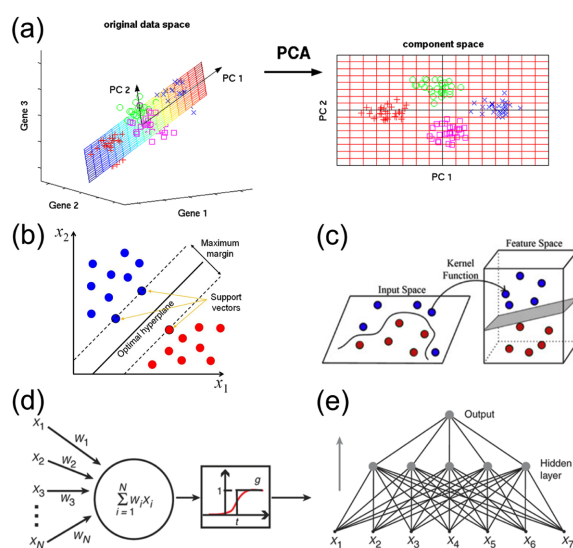

Fig 3. Basic machine learning (ML) techniques. (a) Principal component analysis (PCA). Illustrated is the transformation of PCA which reduces many variables to lesser number of new variables termed principal components. 3D samples are projected onto a two-dimensional component space that maintains the largest variance in the data [23]. (b) Support vector machine (SVM). Maximum margin and optimal hyperplane for an SVM trained with samples from two classes. Samples determining the margin are called support vectors. (c) A conceptual depiction of the "kernel trick," which involves transforming raw, input data to a high-dimensional feature space by way of a "similarity" function with corresponding kernel matrix [21]. (d) Graphical representation of the McCulloch-Pitts model neuron or threshold unit for ANN. The total input to a unit is the weighted sum over all inputs, $\Sigma_{i=1}^{N} W_i X_i = W_1 X_1 + W_2 X_2 + ... + W_N X_N$. If this were below a threshold t, the output of the unit would be 1, and 0 otherwise [22]. (e) Feed-forward network. The network shown takes seven inputs and has five units in the hidden layer and one output. It is said to be a two-layer network because the input layer does not perform any computations and is not counted.

extraction, and data visualization [19]. PCA is defined as an orthogonal linear transformation of the data into a new coordinate system, known as the principal subspace, such that the variance of the projected data is maximized on the first coordinate (called the first principal component), the second highest variance on the second coordinate, and so on (Fig. 3a) [19]. A new set of dimensions can be obtained from eigenvectors of the covariance matrix of the data. The eigenvalues of the covariance matrix are the variances of the principal components. The eigenvector with the largest eigenvalue (or variance) is known as the first principal component. A large variance on the first principal component means that data vary significantly across this dimension, which can be easily classified [20].

The dimensionality of the data is determined by the number of

sensors in an array. For example, an array with five sensors produces a five-dimensional space. However, the dimensionality can be reduced to two or three, useful for humans in terms of visualization, by choosing the dimensions that account for over 95% of the total variance [20]. PCA works well for data with high correlation between variables (i.e., cross-reactive sensors) by converting data into a new coordinate system that has a set of orthogonal vectors.

3.2 Support vector machine

A support vector machine (SVM) is a supervised learning method used for the regression and classification tasks [21]. The objective of the SVM is to find a hyperplane that classifies the data points (Fig. 3b). The hyperplane separates all the data points that belong to one class from another. For 2D data, a hyperplane is a straight line, while, for three-dimensional (3D) data, it is a 2D subspace (or plane). Subsequently, this hyperplane can be used to determine the class for unknown data. The data points closest to the hyperplane are known as support vectors. The training of an SVM operates by maximizing the distance (i.e., the "margin") between the support vectors and hyperplane. The larger the margin, the more confident the prediction. If the data is non-linearly separable, a kernel function is used to transform the original data into a higher-dimensional feature space, where the data can be linearly separated (Fig. 3c).

3.3 Artificial neural networks

Artificial neural networks (ANNs) are inspired by the networks of biological neurons in the brain so that the computer can learn about the information presented to solve many types of problems [22]. Each model neuron consists of input and output units (Fig. 3d). The weighted sum of the inputs is passed through the activation function that transfers the result to the output unit. A bias term is also often included in this sum. If the weighted sum exceeds a certain threshold, the neuron fires so that the output of the neuron is 1, otherwise 0. In biological neurons, each connection between the neurons is determined by the strength of a synapse, which corresponds to the weight denoted by the coefficient W_i in Fig. 3d. A multi-layer network is formed by connecting the output of one neuron to the input of another neuron (Fig. 3e). The training of a neural network is usually performed by adjusting the weights and biases to produce the output of the network (predicted value) similar to the target output (actual value). These adjustments operate in such a way that the error,

defined as the difference between the predicted output and the target output, is reduced using the backpropagation algorithm [19]. ANNs can be used for both classification problems with binary outputs (0 and 1) and regression problems with continuous outputs.

4. DATA ANALYSIS BASED ON ML

In this section, several examples of ML-enabled data analysis for FET-based chemical and biological sensors are presented. The ML algorithms include PCA, SVM, and ANN, which were briefly discussed in the previous section.

4.1 PCA-based analysis

Jiang et al. fabricated an array of chemiresistive gas sensors made of sub-100-nm wide conducting polymer nanowires using nanoscale soft lithography [24]. Poly(3,4-ethylene-dioxythiophene)-poly(styrene sulfonate) (PEDOT:PSS) nanowires were functionalized with different self-assembled monolayers (SAMs) to identify volatile organic compounds (VOCs) at a low concentration range (Fig. 4a). The side chains and functional groups of the SAMs generated a distinct response pattern of each target analyte. The measured pattern from the gas sensor array was used for PCA analysis to classify ten VOC vapors, including ketones, alcohols, alkanes, aromatics, and amines, as shown in Figs. 4b and 4c. The researchers further used the multivariate linear regression method to predict acetone concentration against the actual level in the range of 800 to 2000 ppm with a low average error of 2.97 ppm.

Kim et al. used an electrospinning method to synthesize catalyst-loaded one-dimensional semiconductor metal oxide nanofibers as sensing materials for chemiresistive type breath sensors to detect potential biomarkers of certain diseases, including those of hydrogen sulfide, acetone, and toluene in exhaled breath [25]. Interfering analytes were hydrogen, ethanol, carbon monoxide, ammonia, methane, pentane, and methyl mercaptan. The PCA analysis showed that both individual biomarker species and mixture gases were successfully identified without overlapping with each other. In addition, the PCA analysis clearly classified the simulated halitosis breath and the exhaled breath collected from healthy people into two separate clusters.

Wiederoder et al. developed a cross-reactive array of chemiresistive sensors composed of polymer-graphene nanoplatelet (GNP) composite coated electrodes to detect and discriminate
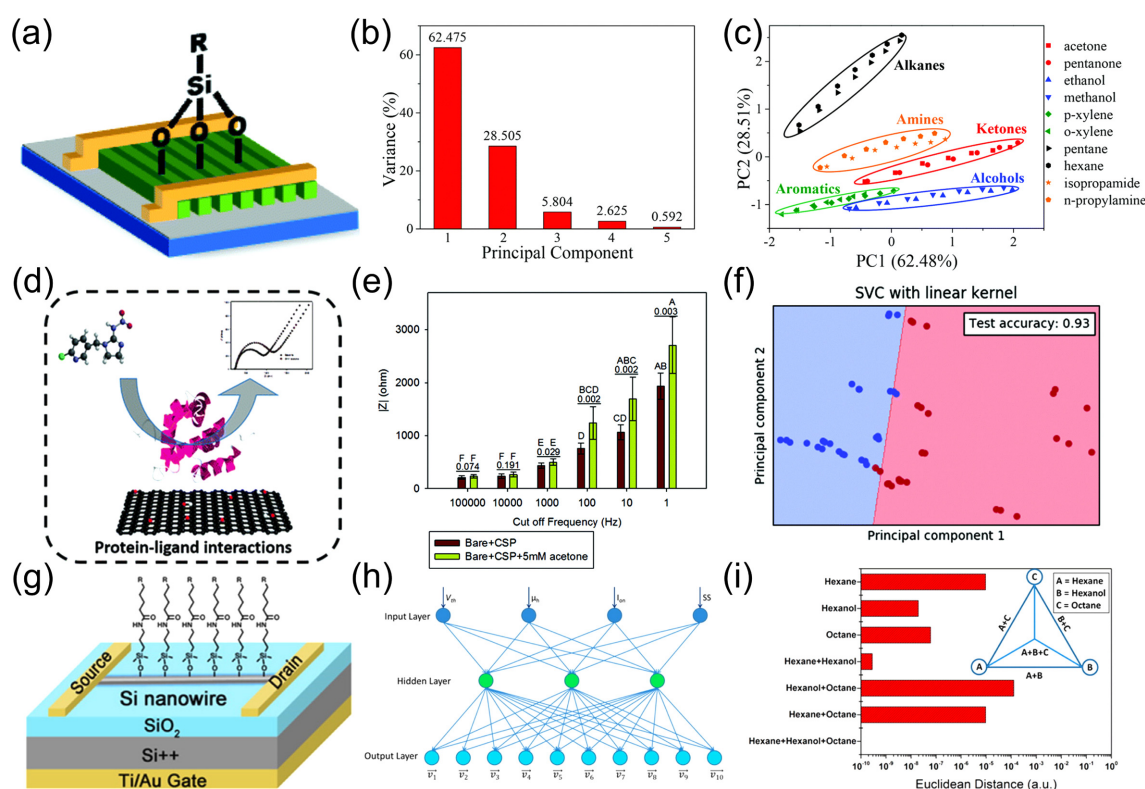
Fig. 4. Data analysis based on machine learning. (a) A schematic of the SAM functionalized PEDOT: PSS nanowires chemiresistor [24]. (b) Screen plot of the principal component analysis. (c) PC2 plotted against PC1 for the sensor array to 5 types of VOCs with seven different concentrations ranging from 800 ppm to 2000 ppm. (d) A schematic of the impedimetric biosensor functionalized with insect-derived chemosensory proteins (CSP) to analyze weak/reversible interactions [27]. (e) Net impedance at representative cut-off frequencies of CSP–acetone interactions in the presence and absence of 5 mM acetone. (f) SVM classification for CSP–acetone biosensors using linear kernel (test accuracy = 96%). Blue dots represent baseline EIS signals (no acetone in samples) and red dots represent positive EIS signals (5 mM acetone in samples). The decision surface of the SVM classifier is plotted by red and blue regions. (g) Scheme of a molecularly modified SiNW FET sensor. [30]. (h) Schematic illustration of an ANN model for VOC recognition. (i) Euclidean distance of ANN outputs using the sensor functionalized with –COOCH$_3$ to identify hexane, hexanol, octane, and their binary and ternary mixtures. Inset: Schematics of the relationship among single VOCs and their binary and ternary mixtures in ANN outputs.

chemical warfare agents (CWAs) [26]. The array of 12 sensors, each functionalized with a different polymer-GNP composite, was exposed 100 times to single analyte vapors, including 5 chemically similar CWA simulants and 8 interfering gases. After some data preprocessing to reduce the effects of concentration, as well as noise, the measured data were dimensionally reduced using PCA, and the first three principal components were selected for classification. For all analytes, CWA simulants, and interferents, the accuracy of four ML algorithms (k-nearest neighbors, support vector classifier, random forest, and linear discrimination analysis) was in the range of 89-100%.

4.2 SVM-based analysis

Rong et al. utilized an SVM classifier to detect acetone, an important biomarker related to diabetic ketoacidosis, using

impedimetric biosensors functionalized with insect-derived chemosensory proteins (Fig. 4d) [27]. The addition of clinically relevant acetone to the receptor-functionalized electrode caused only a slight difference (Fig. 4e). Weak/reversible interactions between small molecules and proteins are a major challenge. To address the problem, they extracted 152 features from both real and imaginary impedance at frequencies ranging from 100 kHz to 1 Hz, which could be further reduced to a 2D principal-components matrix at the 95% confidence interval using the PCA technique. The SVM exhibited an accuracy of 95 ± 4% in cross validation and prediction of test samples (Fig. 4f).

Horsfall *et al.* prepared an array of seven heterojunction semiconducting metal oxide sensors (i.e., unmodified, admixed and 2-layered sensors) consisting of tungsten trioxide (WO$_3$) and chromium titanium oxide to detect explosive gases [28]. The 2-layered sensors showed higher sensitivity in response to ethanol,

ammonia, and nitromethane. The admixed sensors exhibited high sensitivity when exposed to nitrogen dioxide. Because a single sensor does not provide the selectivity needed for the detection of explosives, an SVM algorithm based on an array of seven sensors was used to demonstrate the selectivity. The sensor array produced a dataset of 840 vectors, which included the maximum responses to each gas at given concentrations, initial change in resistivity, and sensor temperature. The SVM algorithm classified the four gases with 71.4% accuracy.

Bian *et al*. demonstrated carbon-nanotube-based FETs as sensor devices to discriminate five purine compounds—adenine, guanine, xanthine, uric acid, and caffeine [29]. One NTFET device was left bare, and four NTFET devices were decorated with metal nanoparticles (Au, Pt, Pd, and Rh). For an SVM analysis, features were extracted from the transfer characteristics of the NTFET devices cross-sensitive to the analytes. The selected eleven features were: the relative change in transconductance (slope), threshold voltage shift, relative changes in conductance at $V_G = 0.6$ V and -0.6 V, changes in overall conductance at $V_G = 0.6$ V, 0.4 V, 0.3 V, -0.3 V, -0.4 V, and -0.6 V normalized to conductance at the threshold voltage, and relative change in minimum conductance. Their approach detected caffeine with 93.4% accuracy. Among the features, transconductance, threshold voltage, and minimum conductance were the most crucial features for overall classification. Density functional theory calculations verified that the selected parameters are associated with the charge transfer between analyte molecules and carbon nanotubes.

4.3 ANN-based analysis

Wang *et al*. reported a combined method based on silcon nanowire (SiNW) FETs and ANN models to selectively identify VOCs (Fig. 4g) [30]. Instead of array of different sensors, they utilized a molecularly modified SiNW FET that produces multiple device parameters (threshold voltage, hole mobility, subthreshold swing, and on-state current) as input to ANN models (Fig. 4h). This approach showed high selectivity toward specific VOCs in both single-component and multi-component mixtures (Fig. 4i). In addition, the VOC concentrations could be predicted with mean prediction errors less than 10%.

Nakhleh *et al*. demonstrated an array of cross-reactive sensors composed of a random network of single-walled carbon nanotubes and molecularly modified gold nanoparticles to analyze exhaled breath [31]. This sensor array was used for the evaluation of a total of 2808 breath samples collected from 1404 subjects having one of 17 different disease types and health controls. Four

numerical sensing features were extracted: the relative change in the sensor's resistance at the beginning, middle, and end of the exposure, as well as the area under the curve of the whole measurement. The overall patterns of the sensing features had discriminative characteristics among the diseases. A series of discriminant factor analysis (DFA) binary classifiers were built with combinations of sensitive sensors to identify the different diseases from one another. The average accuracy of the DFA binary classifiers was 86%.

Kim *et al*. fabricated the sensor array with carboxylated single-walled carbon nanotubes with a range of eight pH values (1.9 to 12.1) to detect NH_3 and CO_2 gases [32]. The resistances of the 16-channel sensor array were recorded upon exposure to the target gas. Adjusting the pH value led to orthogonal sensor responses toward NH_3 and CO_2: the sensor at pH 1.9 showed strong positive responses to NH_3, and the sensor at pH 9.1 exhibited negative responses only to CO_2. Feature vectors were extracted from raw data, and processed data, from the 16-channel sensor array. Subsequently, a neural network model was used to predict NH_3 and CO_2 concentrations. The model was trained for approximately 500 epochs using 70% of the data, 1/3 of which were used for cross validation. The trained model produced loss (i.e., the mean squared logarithmic error) of 0.026 when evaluated against the test set. The predicted values of NH_3 and CO_2 concentrations were well correlated with the exposed (true) values of the test set.

5. SENSOR DESIGN BASED ON ML

5.1 FET design

The performance of chemical and biological sensors based on FETs is related to the electrical characteristics of FET itself [18]. The voltage, current, and normalized current signals are correlated with capacitive coupling, transconductance, and subthreshold swing, respectively [33].

Since many process factors alter the device performance, choosing the optimal conditions is important to fabricate high-performance sensors. Cao *et al*. reported how Design of Experiments (DoE) combined with ML can optimize several variables affecting the device performance and accelerate the process of optimization[34]. In the first round, a fraction factorial design (based on a Latin square sampling technique), instead of a full factorial design, was used to find areas of interest for further optimization (Fig. 5a). The measured data (i.e., the power conversion efficiency from solar cells) were fitted with an SVM
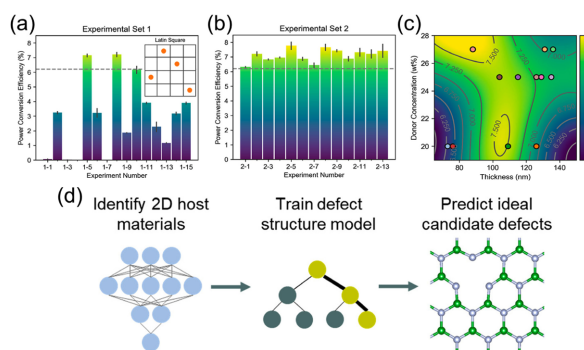
Fig. 5. Sensor design based on ML. Mean power conversion efficiency (PCE) of the solar cells from the first (a) and second (b) rounds of optimization [34]. Inset: An example of factorial sampling in 2-factor 4-value system showing Latin square. (c) Radial basis function visualization of measured cell power conversion efficiency versus thickness and donor concentration of the solar devices. (d) Schematic of the entire workflow for design of point defects in 2D materials. Deep transfer learning is used to predict 2D host material properties and identify promising hosts, a random forest ML model is trained to predict defect structure properties, and finally ideal candidate defects are predicted [39].

to visualize the effects of experiment parameters on the device performance. In the second (subsequent) round of parameter evaluation (Fig. 5b), the ranges of each of the parameters were narrowed, and the corresponding data were fitted with the SVM to find the optimum value of the output performance (Fig. 5c). These ML fitting methods can be beneficial in saving time and resources to design the FET-based sensors.

2D monolayers of semiconducting transition metal dichalcogenides (TMDCs) are considered promising sensing materials owing to their atomic structure, allowing efficient conversion of binding effect at the surface into electrical signals[35]. Due to weak interlayer Van der Waals interaction, a bulk type of TMDCs is mechanically or chemically exfoliated into a monolayer. The electrical characteristics of monolayer TMDCs, which potentially affect the sensor performance, can be modulated with two common methods: 1) introduction of defects on the surface [36] and 2) stacking of layered material[37]. Defects in 2D materials are highly sensitive to local conditions, making them suitable for chemical and biological sensing [38]. Frey *et al*. identified optimal point defects in 2D materials using a combination of ML algorithms and first-principles calculations (Fig. 5d) [39]. In the study, deep transfer learning was used to predict critical host material properties (i.e., band gap and formation energy) and identify promising hosts. A random forest ML model was then trained to predict the defect structure properties that are referenced

to first-principles calculations. Although ideal candidate defects were predicted for quantum emission and resistive switching, a similar ML-enabled design will be utilized for sensor applications. Vertically stacked 2D layers allow making a new type of hybrid material with unprecedented electronic, transport, optical, and mechanical properties [37,40]. Bassman *et al*., utilized ML algorithms for accelerated design of layered materials [41]. Gaussian process regression model was used to predict material properties (i.e., the electronic band gap and conduction/valence band dispersions) of an input heterostructure (e.g., $MoSe_2WTe_2 MoS_2$), and a type of active learning called Bayesian optimization was then used to design the optimal heterostructure. The models have potential to discover ideal 2D heterostructure candidates for sensor applications.

Organic FETs (OFETs) have the advantage to be used as sensing platforms owing to their mechanical flexibility, solution-based low-cost fabrication, and easy chemical functionalization [42]. In the work conducted by Lee [43], ML was trained with the experimentally available data on electron mobility of n-type OFETs to identify the effects of electronic properties on electron mobility. Two ML algorithms, random forest and gradient boosting, were used to construct the ML regression models based on the dataset consisting of input variables (i.e., HOMO levels and LUMO levels) and target variable (i.e., electron mobility). With the fact that the electron mobility is directly related to the current signal of FET-based sensors [33], improving the electronic mobility of FETs via ML algorithms can contribute to a design of sensitive FET-based sensors.

5.2 Receptor design

Finding a specific receptor for a target molecule helps design sensors with better sensitivity and selectivity. Engineered catalysts, enzymes, and receptors predicted by ML enable enhanced chemical and biological reactions on the sensor surface, which is further amplified with sensitive electronic devices mentioned in Section 5.1. Compared with widely used strategies for enzyme engineering such as model-driven rational design and directed evolution, this ML-based design can predict new, previously unseen but promising enzymes, by analyzing the patterns in the collected data [44]. In the study conducted by Song *et al*., ML-based classification is used to discover aptamers, a class of single strand DNA/RNA capable of specific molecular recognition of their targets, with high accuracy and efficiency [45]. Design of aptamers with ligand-induced conformational change near the FET surface is critical to overcome limitations in detection of

small target molecules [46].

6. CONCLUSIONS

Electronic transduction of chemical and biological reaction enables an FET to possess label-free and sensitive detection as a sensor. ML with the ability to learn from data and predict output allows researchers to analyze complex signals generated by sensors and design high-performance sensors. Supervised and unsupervised ML algorithms, including PCA, SVM, and ANN, were utilized to classify unknown substances and quantify the concentration of target molecules. ML combined with DoE is also used to predict the electrical characteristics of electronic devices for accelerating the sensor design by saving time and resources. A similar ML-based approach can be applied to receptor design to achieve high sensitivity and selectivity.

There remain several challenges of the combination of sensors and ML. Usually, data are analyzed using ML algorithms installed on a computer, outside the sensor platform, limiting the sensor portability. To address this problem, innovative methods for seamless integration of sensors and ML hardware should be developed [47,48]. Sufficient "big data" is required to train ML, and it is quite well worked out in gas sensing experiments where the reversible reaction allows chemical sensors to be used many times. A biosensor based on reversible reaction between receptors and targets is considered a sensing platform suitable for ML-based analysis to collect sufficient data for training, with limited time and resources [27].

ACKNOWLEDGMENT

REFERENCES

[1] M. Kaisti, "Detection principles of biological and chemical FET sensors", *Biosens. Bioelectron.,* Vol. 98, pp. 437-448, 2017.

[2] T. Lee *et al.*, "Recent advances in AIV biosensors composed of nanobio hybrid material", *Micromachines,* Vol. 9, No. 12, pp. 651, 2018.

[3] T. Lee *et al.*, "Development of the Troponin Detection System Based on the Nanostructure", *Micromachines,* Vol. 10, No. 3, pp. 203, 2019.

[4] M.-Z. Li, S.-T. Han, and Y. Zhou, "Recent Advances in Flexible Field-Effect Transistors toward Wearable Sensors", *Adv. Intell. Syst.,* Vol. 2, No. 11, pp. 2000113, 2020.

[5] Y. LeCun, Y. Bengio, and G. Hinton, "Deep learning", *Nature,* Vol. 521, No. 7553, pp. 436-444, 2015.

[6] A. F. de Almeida, R. Moreira, and T. Rodrigues, "Synthetic organic chemistry driven by artificial intelligence", *Nat. Rev. Chem.,* Vol. 3, No. 10, pp. 589-604, 2019.

[7] Y. Gil, M. Greaves, J. Hendler, and H. Hirsh, "Amplify scientific discovery with artificial intelligence", *Science,* Vol. 346, No. 6206, pp. 171-172, 2014.

[8] K. A. Brown, S. Brittman, N. Maccaferri, D. Jariwala, and U. Celano, "Machine Learning in Nanoscience: Big Data at Small Scales", *Nano Lett.,* Vol. 20, No. 1, pp. 2-10, 2019.

[9] Y. Cui, Q. Wei, H. Park, and C. M. Lieber, "Nanowire nanosensors for highly sensitive and selective detection of biological and chemical species", *Science,* Vol. 293, No. 5533, pp. 1289-1292, 2001.

[10] E. Stern *et al.*, "Label-free immunodetection with CMOS-compatible semiconducting nanowires", *Nature,* Vol. 445, No. 7127, pp. 519-522, 2007.

[11] M. A. H. Khan and M. V. Rao, "Gallium Nitride (GaN) Nanostructures and Their Gas Sensing Properties: A Review", *Sensors,* Vol. 20, No. 14, pp. 3889, 2020.

[12] Q. Liu *et al.*, "Highly sensitive and quick detection of acute myocardial infarction biomarkers using In2O3 nanoribbon biosensors fabricated using shadow masks", *ACS Nano,* Vol. 10, No. 11, pp. 10117-10125, 2016.

[13] A. K. Wanekaya, M. A. Bangar, M. Yun, W. Chen, N. V. Myung, and A. Mulchandani, "Field-effect transistors based on single nanowires of conducting polymers", *J. Phys. Chem. C,* Vol. 111, No. 13, pp. 5218-5221, 2007.

[14] J. Kwon *et al.*, "Nanoscale FET-based transduction toward sensitive extended-gate biosensors", *ACS Sens.,* Vol. 4, No. 6, pp. 1724-1729, 2019.

[15] J.-H. Ahn, J. Yun, Y.-K. Choi, and I. Park, "Palladium nanoparticle decorated silicon nanowire field-effect transistor with side-gates for hydrogen gas detection", *Appl. Phys. Lett.,* Vol. 104, No. 1, pp. 013508, 2014.

[16] Y. G. Song, G. S. Kim, B.-K. Ju, and C.-Y. Kang, "Design of Semiconducting Gas Sensors for Room-Temperature Operation", *J. Sens. Sci. Technol.,* Vol. 29, No. 1, pp. 1-6, 2020.

[17] I. Lundström, S. Shivaraman, C. Svensson, and L. Lundkvist, "A hydrogen− sensitive MOS field− effect transistor", *Appl. Phys. Lett.,* Vol. 26, No. 2, pp. 55-57, 1975.

[18] P. R. Nair and M. A. Alam, "Design considerations of silicon nanowire biosensors", *IEEE Trans. Electron Devices,* Vol. 54, No. 12, pp. 3400-3408, 2007.

[19] C. M. Bishop, *Pattern recognition and machine learning,* Springer, 2006.

[20] Z. Li, J. R. Askim, and K. S. Suslick, "The optoelectronic nose: colorimetric and fluorometric sensor arrays", *Chem. Rev.,* Vol. 119, No. 1, pp. 231-292, 2018.

[21] D. A. Pisner and D. M. Schnyer, "Support vector machine" ,in *Machine Learning*: Elsevier, 2020, pp. 101-121.

[22] A. Krogh, "What are artificial neural networks?", *Nat. Biotechnol.,* Vol. 26, No. 2, pp. 195-197, 2008.

[23] M. Scholz, *Approaches to analyse and interpret biological profile data*, University of Potsdam, Germany, Ph.D. thesis, 2006.

[24] Y. Jiang, N. Tang, C. Zhou, Z. Han, H. Qu, and X. Duan, "A chemiresistive sensor array from conductive polymer nanowires fabricated by nanoscale soft lithography", *Nanoscale,* Vol. 10, No. 44, pp. 20578-20586, 2018.

[25] S.-J. Kim, S.-J. Choi, J.-S. Jang, H.-J. Cho, and I.-D. Kim, "Innovative nanosensor for disease diagnosis", *Acc. Chem. Res.,* Vol. 50, No. 7, pp. 1587-1596, 2017.

[26] M. S. Wiederoder *et al.*, "Graphene nanoplatelet-polymer chemiresistive sensor arrays for the detection and discrimination of chemical warfare agent simulants", *ACS Sens.,* Vol. 2, No. 11, pp. 1669-1678, 2017.

[27] Y. Rong *et al.*, "Post hoc support vector machine learning for impedimetric biosensors based on weak protein–ligand interactions", *Analyst,* Vol. 143, No. 9, pp. 2066-2075, 2018.

[28] L. A. Horsfall, D. C. Pugh, C. S. Blackman, and I. P. Parkin, "An array of WO3 and CTO heterojunction semiconducting metal oxide gas sensors used as a tool for explosive detection", *J. Mater. Chem. A,* Vol. 5, No. 5, pp. 2172-2179, 2017.

[29] L. Bian *et al.*, "Machine-Learning Identification of the Sensing Descriptors Relevant in Molecular Interactions with Metal Nanoparticle-Decorated Nanotube Field-Effect Transistors", *ACS Appl. Mater. Interfaces,* Vol. 11, No. 1, pp. 1219-1227, 2018.

[30] B. Wang, J. C. Cancilla, J. S. Torrecilla, and H. Haick, "Artificial sensing intelligence with silicon nanowires for ultraselective detection in the gas phase", *Nano Lett.,* Vol. 14, No. 2, pp. 933-938, 2014.

[31] M. K. Nakhleh *et al.*, "Diagnosis and classification of 17 diseases from 1404 subjects via pattern analysis of exhaled molecules", *ACS Nano,* Vol. 11, No. 1, pp. 112-125, 2017.

[32] B. Kim, T. J. Norman, R. S. Jones, D.-I. Moon, J.-W. Han, and M. Meyyappan, "Carboxylated Single-Walled Carbon Nanotube Sensors with Varying pH for the Detection of Ammonia and Carbon Dioxide Using an Artificial Neural Network", *ACS Appl. Nano Mater.,* Vol. 2, No. 10, pp. 6445-6451, 2019.

[33] J.-H. Ahn, B. Choi, and S.-J. Choi, "Understanding the signal amplification in dual-gate FET-based biosensors", *J. Appl. Phys,* Vol. 128, No. 18, pp. 184502, 2020.

[34] B. Cao *et al.*, "How to optimize materials and devices via design of experiments and machine learning: Demonstration using organic photovoltaics", *ACS Nano,* Vol. 12, No.

[35] S. Manzeli, D. Ovchinnikov, D. Pasquier, O. V. Yazyev, and A. Kis, "2D transition metal dichalcogenides", *Nat. Rev. Mater.,* Vol. 2, No. 8, pp. 17033, 2017.

[36] Z. Lin *et al.*, "2D materials advances: from large scale synthesis and controlled heterostructures to improved characterization techniques, defects and applications", *2D Mater.,* Vol. 3, No. 4, pp. 042001, 2016.

[37] A. K. Geim and I. V. Grigorieva, "Van der Waals heterostructures", *Nature,* Vol. 499, No. 7459, pp. 419-425, 2013.

[38] T. Hussain, T. Kaewmaraya, S. Chakraborty, and R. Ahuja, "Defect and substitution-induced silicene sensor to probe toxic gases", *J. Phys. Chem. C,* Vol. 120, No. 44, pp. 25256-25262, 2016.

[39] N. C. Frey, D. Akinwande, D. Jariwala, and V. B. Shenoy, "Machine Learning-Enabled Design of Point Defects in 2D Materials for Quantum and Neuromorphic Information Processing", *ACS Nano,* Vol. 14, No. 10, pp. 13406-13417, 2020.

[40] C.-H. Lee *et al.*, "Atomically thin p–n junctions with van der Waals heterointerfaces", *Nat. Nanotechnol.,* Vol. 9, No. 9, pp. 676, 2014.

[41] L. Bassman *et al.*, "Active learning for accelerated design of layered materials", *npj Comput. Mater.,* Vol. 4, No. 1, pp. 1-9, 2018.

[42] P. Lin and F. Yan, "Organic thin-film transistors for chemical and biological sensing", *Adv. Mater.,* Vol. 24, No. 1, pp. 34-51, 2012.

[43] M. H. Lee, "Machine Learning for Understanding the Relationship between the Charge Transport Mobility and Electronic Energy Levels for n-Type Organic Field-Effect Transistors", *Adv. Electron. Mater.,* Vol. 5, No. 12, pp. 1900573, 2019.

[44] S. Mazurenko, Z. Prokop, and J. Damborsky, "Machine learning in enzyme engineering", *ACS Catal.,* Vol. 10, No. 2, pp. 1210-1223, 2019.

[45] J. Song *et al.*, "A Sequential Multidimensional Analysis Algorithm for Aptamer Identification based on Structure Analysis and Machine Learning", *Anal. Chem.,* Vol. 92, No. 4, pp. 3307-3314, 2019.

[46] N. Nakatsuka *et al.*, "Aptamer–field-effect transistors overcome Debye length limitations for small-molecule sensing", *Science,* Vol. 362, No. 6412, pp. 319-324, 2018.

[47] Y. Kim *et al.*, "A bioinspired flexible organic artificial afferent nerve", *Science,* Vol. 360, No. 6392, pp. 998-1003, 2018.

[48] C. Wan *et al.*, "An artificial sensory neuron with tactile perceptual learning", *Adv. Mater.,* Vol. 30, No. 30, pp. 1801291, 2018.